Conference on Modelling Fluid Flow (CMFF'25)
The 19th International Conference on Fluid Flow Technologies
Budapest, Hungary, August 26-August 29, 2025

MODELLING THE TRANSPORT OF OXYGEN IN THE HUMAN VASCULAR SYSTEM

Márta VIHAROS[1], Richárd WÉBER[2], György PAÁL[3]

[1] Department of Hydrodynamic Systems, Faculty of Mechanical Engineering, Budapest University of Technology and Economics. H-1111 Budapest, Műegyetem rkp. 3., Hungary. Corresponding Author. E-mail: viharos.marti@gmail.com
[2] Department of Hydrodynamic Systems, Faculty of Mechanical Engineering, Budapest University of Technology and Economics. H-1111 Budapest, Műegyetem rkp. 3., E-mail: rweber@hds.bme.hu
[3] Department of Hydrodynamic Systems, Faculty of Mechanical Engineering, Budapest University of Technology and Economics. H-1111 Budapest, Műegyetem rkp. 3., E-mail: gypaal@hds.bme.hu

ABSTRACT

Low-dimensional hemodynamic simulations offer the advantage of modelling blood flow across the entire vascular system simultaneously. This approach enables the representation of large-scale physiological processes, including the complete cycle of oxygen transport within the vascular system.

In this cycle, inhaled oxygen diffuses from the alveoli into the pulmonary capillaries. Oxygenated blood is then transported via the pulmonary veins to the left heart and subsequently distributed through the systemic arteries. In the systemic capillaries, oxygen diffuses from the blood plasma into the surrounding tissues. The resulting deoxygenated blood is returned to the right heart through the systemic veins and is then transported back to the lungs via the pulmonary arteries. These processes involve advection-driven blood transport between two diffusion-driven stages: oxygen uptake in the lungs and oxygen delivery to tissues. The heart sustains this cycle by providing the necessary energy to maintain blood flow.

The primary objective of this study is to simulate these processes and replicate a realistic oxygen transport cycle within the whole modeled vascular system using the one- and zero-dimensional hemodynamic solver, first_blood. Evaluation of the simulation results demonstrated that the model successfully reproduces realistic dynamics across the entire vascular system.

Keywords: tissue oxygenation, oxygen uptake, hemodynamics, one- and zero-dimensional simulations

NOMENCLATURE

A	Cross section $[m^2]$
C	Oxygen concentration $\left[\frac{m^3}{m^3}\right]$
D	Diffusion coefficient $\left[\frac{m^3}{m^3}\right]$
$K_{\max}$	- $\left[\frac{m^3(O_2)}{m^3(\text{plasma})\cdot mmHg\cdot s}\right]$
$M_{\max}$	Maximum consumption rate of oxygen $\left[\frac{m^3(O_2)}{s\cdot m^3(\text{plasma})}\right]$
P	Partial pressure $[mmHg]$
h_c	Wall thickness of capillary vessels $[m]$
j	Index of the given division point [1]
n	Number of division points [1]
t	Time $[s]$
x	Axial coordinate $[m]$
α	Oxygen solubility $\left[\frac{m^3}{mmHg\cdot m^3}\right]$
κ	Wall permeability $\left[\frac{m^3(O_2)}{mmHg\cdot mm\cdot s}\right]$
ϕ	Volume fraction [%]
τ	Time constant of oxygen dissolution $[s]$
$\frac{S}{V}$	Vessel surface area to volume $\left[\frac{1}{m}\right]$
C_{RBC}	RBC concentration in blood $\left[\frac{1}{m^3(\text{plasma})}\right]$
HB	Haemoglobin [−]
HB_{O_2}	Haemoglobin saturation [%]
RBC	Red blood cell [−]

Subscripts and Superscripts

a	Alveoli
c	Capillary
p	Pulmonary
sat	Saturation
t	Tissue

1. INTRODUCTION

Studying biological processes through mathematical modeling could become a cornerstone in understanding complex physiological phenomena in the future. Hemodynamics, the dynamics of blood flow, is a fundamental aspect of cardiovascular physiology, directly influencing the delivery of nutrients and oxygen to tissues.

The vascular system has many tasks, one of which is the transport of O_2 (oxygen), which is of

prime importance. O_2 is crucial for the body since human cells need O_2 to produce adenosine triphosphate, which can be used or stored as energy. In case of inadequate blood supply, the body activates certain autoregulation processes to match the demand. For realistic haemodynamic simulations, taking these into account is inevitable.

The simulation of O_2 transport is the first step to simulate certain autoregulation processes, such as the metabolic response. For that reason, this article presents a mathematical model for the O_2 transport. The models include tissue O_2 uptake at the systemic capillaries and blood oxygenation at the pulmonary capillaries. Modelling these two processes ensures that the whole O_2 transport cycle is adequately captured.

1.1. The vascular system model

Low-dimensional haemodynamic simulations have the advantage of being computationally less demanding, making it possible to simulate blood flow in almost the entire vascular system simultaneously. This approach considers each large vessel as an axisymmetric pipeline, which builds up a vascular tree. Two equations describing the behavior of the fluid, the mass and momentum balances, are solved. The vessels are not rigid, so a material model connecting the transmural pressure and vessel deformation is needed [1]. This adds a third independent equation to the previous two. A detailed description of the vascular model is presented in [2]. The three independent equations are solved with the MacCormack scheme and the method of characteristics with the first_blood solver [3, 4].

1.2. Structure of the paper

The paper is structured as follows: After the introduction, a model for transport simulation in lumped models is presented. This is followed by a description of a modified version of the tissue oxygenation model from [5]. Before the results are presented and discussed, the blood oxygenation model is also introduced.

2. METHODS

2.1. Transport model for lumped models

For the vessels modelled in one dimension, the transport equation is solved given by Eq. 1, where C is a general transport variable. The effect of diffusion is small compared to the advection, the minimum of the Péclet number is around $P_{e_{O_2}} = \frac{v_c L_c}{D_{O_2}} = \frac{0.001[\frac{m}{s}] \cdot 0.00315[m]}{1.65 \cdot 10^{-9}[\frac{m^2}{s}]} \approx 1909$[1], where v_c is velocity of the plasma in the capillaries [6], L_c is the length of a capillary (the value is estimated) and D_{O_2} is the diffusion coefficient [5]. Red blood cells are much larger than O_2 molecules, and the effect of diffusion is even smaller, so the diffusion along the vessel axis can be neglected entirely.

The solver calculates the velocity field in every timestep for all vessels; thus, the concentration values can also be determined. At the intersections of the vessels there are nodes, the concentration is determined by assuming perfect mixing, providing boundary conditions. The concentration of the nodes is calculated as the weighted average of concentrations flowing toward the node, and the weights are the volumetric flow rates.

$$\frac{\partial C}{\partial t} = -v\frac{\partial C}{\partial x} \tag{1}$$

Besides the vessels modelled in 1D, there are also lumped models. For example, the peripherals are modelling small vessels, veins and organs. The structure of a peripheral model can be seen in Figure 1. The solver determines the volumetric flow rate and pressure values for these zero-dimensional models in each time step. Velocity and a spatial coordinate are necessary to calculate the transport. The next description briefly describes how these parameters are estimated for the 0D models.

- The time average of the volumetric flow rate corresponding to the resistance at the given peripheral model is calculated from a previous simulation for a cardiac cycle.
- Average velocity values corresponding to each segment can be found in the literature [6]. Time and spatial averages are needed in the simulations for arterioles, capillaries, venules, and veins. Table 1 presents the literature values considered in this work.
- The flow rate and the velocity determine the cross-section area for each segment. This way, in every time step with the previously calculated volumetric flow rate, a realistic velocity value can be obtained.
- Finally, the length is estimated for each segment; see Table 1 for the values. The venous vessel lengths are assumed to be equal to the length of the arterial path from the heart to the considered periphery.

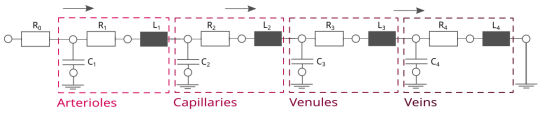

Figure 1. Peripheral models. Each compartment (arterioles, capillaries, venulares and veins) is modeled with an RLC circuit [7]. The left node of the lumped model is connected to a 1D vessel segment.

Providing that all segments at each periphery have every necessary additional parameter (a cross-section area and length), the transport of substances

Table 1. Velocity and length values for each segment. * indicates that for each peripheral model, the sum of the venous vessel lengths is uniquely determined based on the arterial model. The venous vessel lengths are assumed to be equal to the length of the arterial path from the heart to the considered periphery.

	v $[\frac{m}{s}]$	L $[m]$
arterioles	0.02	0.0225
capillaries	0.001	0.00315
venules	0.033	0.00515
veins	0.133	*

can be simulated the same way as for the vessels modelled in one dimension. The described transport model is general, and an arbitrary number of transport variables can be solved simultaneously.

2.2. Tissue oxygenation

The haemoglobin (HB) in red blood cells (RBCs) is mainly responsible for oxygen delivery. An HB molecule can bind a maximum of four O_2 molecules reversibly. Hemoglobin saturation (HB_{sat}) indicates the percentage of bound O_2 molecules relative to the maximum amount possible. If all HB molecules are bound to four O_2 molecules, the saturation is 100%. O_2 molecules stay attached to the HB molecules because of a balance between the partial pressure of O_2, $P_{O_2,p}$, and the HB saturation. This balance can be represented with a sigmoid curve. The curve is obtained by fitting (with the least squares method), while the data points are taken from the relevant interval of $P_{O_2,p}$ ($40mmHg \leq P_{O_2,p} \leq 95mmHg$) from the literature, see Table 2. The function is given by Eq. 2,

$$HB_{O_2} = \frac{L}{1 + e^{-k(P_{O_2} - m)}} + b \tag{2}$$

where $L = 1.251[-]$, $k = 0.0676[1/mmHg]$, $m = 17.71[mmHg]$ and $b = -0.274[-]$, and the curve is shown by Figure 2. The shape of the curve can be explained by the fact that the first O_2 molecule bound to an HB molecule changes the O_2-affinity, making the binding of the second and third O_2 molecule easier [8].

Table 2. Corresponding values of P_{O_2} [mmHg] and HB_{O_2} [1] in normal physiological conditions in the relevant interval ($40mmHg \leq P_{O_2} \leq 95mmHg$

P_{O_2}	40	50	60	70	80	95
HB_{O_2}	0.75	0.85	0.91	0.94	0.96	0.97

As RBC reaches the capillaries, the partial pressure reduces; thus, the O_2 disconnects from the HB molecules and enters the blood plasma. Between the plasma and the tissue, the main driving force is the diffusion because the velocity of plasma is

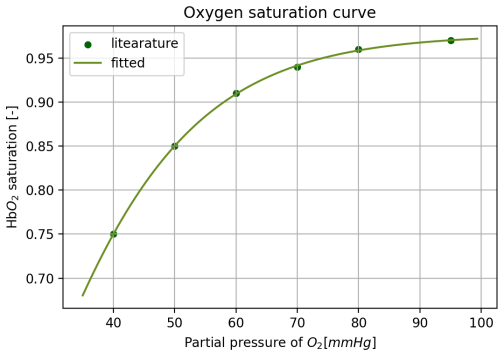

Figure 2. Sigmoid curve fitted with least squares method to data points are taken from Table 2.

$\approx 0.5 - 1[\frac{mm}{s}]$ [6], leaving enough time for the O_2 diffusion from the plasma to tissues through the capillary walls. Altogether, four transport equations are solved to model this complicated phenomenon, one for each: RBC, HB_{O_2}, O_2 concentration in the plasma, and O_2 concentration of the tissue. In larger arteries, arterioles, venules, and veins, O_2 absorption is negligible; thus, Eq. 1 is solved for these parts of the vascular model. However, handling the O_2 diffusion needs special source terms.

Capillaries can be found in the systemic peripherals and also in the pulmonary circulation. First, we discuss the former. The mathematical model describing the tissue oxygenation is based on the work of Bing [5]. The following assumptions are applied in the case of this model:

- O_2 and RBC diffusion is neglected along the vessel axis.
- The dissolution of O_2 from HB to plasma is instantaneous, i.e., Eq. 2 is updated each timestep.
- The inter-segment advection (e.g. arterioles-venules) term is not considered. This means that the partial pressure difference of O_2 between the segments does not inflict a change in O_2 concentration.

All following differential equations are advection transport ones with different source terms to mimic certain biological or chemical effects. The parameters and their values are in Table 3. The first is for the O_2 concentration in the capillaries, C_c, that is

$$\frac{\partial C_c}{\partial t} = \underbrace{-v\frac{\partial C_c}{\partial x}}_{\text{advection}} \underbrace{- \frac{\kappa_c}{h_c}\frac{S_c}{V_c}\left(\frac{C_c}{\alpha_b} - \frac{C_t}{\alpha_t}\right)}_{\text{diffusion from plasma to tissue}} + \underbrace{\frac{1}{\tau}\Delta HB_{O_2} \cdot C_{RBC} \cdot N_{O_2/RBC}\frac{M}{N_A \cdot \rho}}_{O_2 \text{ dissolving from HB to plasma}} \tag{3}$$

The diffusion of O_2 into tissue is driven by the partial pressure difference of dissolved O_2 between the

Table 3. Parameters of tissue oxygenation model. Literature provided an interval for each parameter, and the applied values fall within that range [5]. The exceptions are ϕ_c and $\frac{S_c}{V_c}$, which come from synthetic geometries suggesting different values: $\phi_c = 1.42[\%]$ and $\frac{S_c}{V_c} = 6.1638 \cdot 10^5[\frac{1}{m}]$. ϕ_t is then calculated as 1-ϕ_c.

Notation	Unit	Value
κ_c	$\frac{m^3}{mmHg \cdot mm \cdot s}$	$4.2 \cdot 10^{-14}$
h_c	m	$1.0 \cdot 10^{-6}$
$\frac{S_c}{V_c}$	$\frac{1}{m}$	$4.74 \cdot 10^5$
α_b	$\frac{m^3}{mmHg \cdot m^3}$	$3.11 \cdot 10^{-5}$
α_t	$\frac{m^3}{mmHg \cdot m^3}$	$3.95 \cdot 10^{-5}$
τ	s*	$8.0 \cdot 10^{-2}$
ϕ_c	%	1.1303
ϕ_t	%	98.8697
M_{max}	$\frac{m^3}{s \cdot m^3}$	$2.4 \cdot 10^{-4}$
C_{50}	$\frac{m^3}{mmHg \cdot m^3}$	10^9
$N_{O_2/RBC}$	$\frac{1}{1}$	$2.6 \cdot 10^{-5}$
M	$\frac{kg}{mol}$	0.032
N_A	$\frac{1}{mol}$	$6 \cdot 10^{23}$
ρ	$\frac{kg}{m^3}$	1.43

plasma and the tissue, expressed as $P_{O_2,p} - P_{O_2,t} = \frac{C_c}{\alpha_b} - \frac{C_t}{\alpha_t}$. The term $\frac{\kappa_c}{h_c}\frac{S_c}{V_c}$ represents the rate of change in C_c due to a unit difference in partial pressure. Moreover, the last term models the dissolution of O_2 to plasma from O_2 bound to hemoglobin (HB) according to the following considerations.

- At each timestep there is a given HB_{O_2} and C_c value. These are not necessarily in perfect balance, i.e., the sigmoid relationship given by Eq. 2 is not met. ΔHB_{O_2} gives the difference between the actual state and the sigmoid curve with the current C_c.
- The difference dissolves into the plasma described by the differential equation of a first-order lag.
- The dissolved amount is also substracted from the HB_{O_2} to ensure mass balance.

Eq. (4 describes the O_2 concentration of tissues. The second term, corresponding to the O_2 diffusion from plasma to tissue, is the same as in Eq. (3, but multiplied with $\frac{\phi_c}{\phi_t}$ (the ratio of capillary to tissue volume) and with a different sign to ensure mass balance. The multiplication by $\frac{\phi_c}{\phi_t}$ is necessary since the variables in the equations represent concentration, and the volumes of tissue and blood are different.

$$\frac{\partial C_t}{\partial t} = \underbrace{\frac{\kappa_c}{h_c}\frac{S_c}{V_c}\frac{\phi_c}{\phi_t}\left(\frac{C_c}{\alpha_b} - \frac{C_t}{\alpha_t}\right)}_{\text{diffusion from plasma to tissue}} - \underbrace{\frac{M_{max} C_t}{C_t + C_{50}}}_{O_2 \text{ consumption}}; \quad (4)$$

The O_2 consumption by tissue activity (see last term in Eq. 4) is modelled by the Michaelis–Menten kinetics, where C_{50} is C_t at the half maximum consumption rate [5], as this model is applied to describe nutrient uptake by cells [9].

The third equation describes the HB_{O_2} saturation level. The only source term is the dissolution of O_2 from HB to plasma, same as in Eq. (3).

$$\frac{\partial HB_{O_2}}{\partial t} = \underbrace{-v\frac{\partial HB_{O_2}}{\partial x}}_{\text{advection}} - \underbrace{\frac{1}{\tau}\Delta HB_{O_2}}_{O_2 \text{ dissolving from HB to plasma}} \quad (5)$$

Finally, the last one tracks the flow of RBC cells. As the amount of RBC cells remains constant on the low time scale, no additional source terms exist.

$$\frac{\partial C_{RBC}}{\partial t} = \underbrace{-v\frac{\partial C_{RBC}}{\partial x}}_{\text{advection}} \quad (6)$$

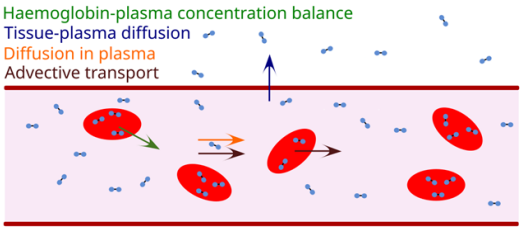

Figure 3. The transport of O_2 in capillaries.

2.3. Blood oxygenation

Gas exchange in the pulmonary circulation occurs with the help of alveoli, which are small air sacs in the lungs that allow gases to enter the blood. The difference between the partial pressure of O_2 in the alveoli and in the capillaries drives the diffusion of O_2. The partial pressure of O_2 in the alveoli is about $P_{O_2,a} = 100[mmHg]$, with minimal fluctuations over time [8]. The applied mathematical method is a modification of the systemic capillaries. The main difference being the direction of O_2 diffusion, and, since the fluctuations of the partial pressure of O_2 in the alveoli is low, it is assumed to be constant, so is the tissue concentration. Overall, there is no need for Eq. 4 in the pulmonary circulation, Eq. 5 and Eq. 6 are the same; however, the development in the source term of the plasma concentration model is crucial to cope the correct O_2 diffusion.

$$\frac{\partial C_{p,c}}{\partial t} = \underbrace{-v\frac{\partial C_{p,c}}{\partial x}}_{\text{advection}} \underbrace{- K_{max} sin^2\left(\frac{j\pi}{n}\right)\left(\frac{C_{p,c}}{\alpha_b} - P_{O_2,a}\right)}_{\text{diffusion from alveoli to plasma}} +$$
$$+ \underbrace{\frac{1}{\tau}\Delta HB_{O_2} \cdot C_{RBC} \cdot N_{O_2/RBC}\frac{M}{N_A \cdot \rho}}_{O_2 \text{ dissolving from HB to plasma}}, j \in \{1; 2...n\}; \quad (7)$$

The second term on the right hand-side of Eq. 7 describes the diffusion of O_2 from the alveoli. K_{max} is a constant parameter representing the maximum concentration change caused by a unit partial pressure difference in one second. The sin^2 function models the gradual change of the vessels rather than a sudden shift, so there is no O_2 diffusion in the start and end of the pulmonary capillaries. $\left(\frac{C_{p,c}}{\alpha_b} - P_{O_2,a}\right)$ is the partial pressure difference driving the diffusion of O_2. Table 4 gives the parameters of Eq. 7.

Table 4. Notations used in Eq. 7 describing the O_2 uptake in the pulmonary capillaries.

Notation	Dimension	(value)
$P_{O_2,a}$	$mmHg$	100
K_{max}	$\frac{m^3}{m^3 \cdot mmHg \cdot s}$	$6.479 \cdot 10^{-4}$

3. RESULTS AND DISCUSSION

Figure 4 represents the results of the O_2 transport simulation. Even though the simulation is transient, it converges to a periodic state. Since the fluctuations of the concentration levels within the periodic state are negligible, the figure contains temporal averages. While the y-axis presents the saturation level and the plasma O_2 concentration for the top- and bottom-side plot, respectively, the x-axis is a quasi-spatial coordinate, i.e., the actual lengths are distorted, giving each segment of the circulatory system the same gap. The HB_{O_2} saturation level (see top-side) is high for the systemic arteries and the pulmonary veins, while it is low for the systemic veins and the pulmonary arteries. The simulation results in a high level of around 97% and a low of 75%, which, as the dashed lines indicate in the figure, match the literature data qualitatively. Similar conclusions can be drawn from the bottom-side figure regarding plasma O_2 concentration. A slight discrepancy is present for the high-oxygenated level, but the low level coincides perfectly. It is interesting to notice the transition from high to low level in both cases. While the saturation level drops linearly, the plasma O_2 concentration shows exponential tendencies.

Even though the model results in physiologically relevant values, the validation can be only considered qualitatively. A significant uncertainty originates from the parameters. Since the original parameters are from different sources, they are not necessarily free from contradictions. The cited article specifically models the human brain, so the parameters determined are not necessarily valid for all body parts. The adopted mathematical model used for the synthetic geometries is given by [10], which focuses solely on the cerebral microvasculature. Some parameters cannot be directly measured, and only estimates can be applied. A patient-specific or even a population-based model needs further in-vivo measurements and calibration of the model. Finally, the modelled biology itself might be more complex than the current model.

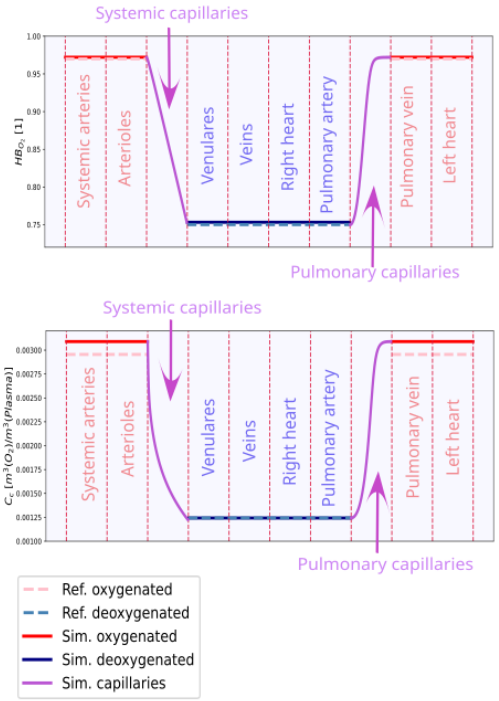

Figure 4. Simulation results of the O_2 transport cycle after the transient. The haemoglobin saturation and plasma O_2 concentration values are physiologically correct at every location in the vascular system.

4. CONCLUSIONS

The paper presents a possible mathematical method to model oxygen (O_2) transport via blood flow in the circulatory system. To obtain the classic hydraulic variables (such as pressure or velocity), the solution of the traditional mass and momentum balance equations and the deformable walls need to be coped. The basis for predicting O_2 concentration is the advection-diffusion equation from fluid dynamics. While diffusion along the vessel axis is negligible due to the high Peclet number, diffusion drives the exchange between the capillaries and tissues in both systemic and pulmonary capillaries. The former provides O_2 for the tissues (such as organs or muscle) using the O_2 for their primary function; the latter is responsible for the O_2 intake to the bloodstream from the lungs.

The presented model is validated qualitatively, i.e., the results coincide with physiological ranges in general. The O_2 saturation level is above 95% after the O_2 intake in the lungs, i.e., the pulmonary veins, the left side of the heart, and the systemic arteries. The O_2 consumption of the tissues at the systemic capillaries reduces O_2 concentration to 75%. However, patient-specific or population-based validation is inevitable in future work, which requires in-vivo measurements performed on real patients. Furthermore,

verification and a thorough uncertainty analysis are necessary to improve the reliability of the model.

ACKNOWLEDGEMENTS

GEMINI has received funding from the European Union's Horizon 2020 research and innovation programme under the grant agreement No 101136438.

The research was supported by the János Bolyai Research Scholarship (BO/00484/23/6) of the Hungarian Academy of Sciences and by the New National Excellence Program of the Ministry for Culture and Innovation from the source of the National Research (Wéber Richárd ÚNKP-22–5-BME-426).

Project no. TKP-6-6/PALY-2021 has been implemented with the support provided by the Ministry of Culture and Innovation of Hungary from the National Research, Development and Innovation Fund, financed under the TKP2021-EGA funding scheme.

REFERENCES

[1] Olufsen, M. S., 1999, "Structured tree outflow condition for blood flow in larger systemic arteries", *American Journal of Physiology-Heart and Circulatory Physiology*, Vol. 276 (1), pp. H257–H268, URL https://www.physiology.org/doi/10.1152/ajpheart.1999.276.1.H257.

[2] Wéber, R., Gyürki, D., and Paál, G., 2023, "First blood: An efficient, hybrid one- and zero-dimensional, modular hemodynamic solver", *International Journal for Numerical Methods in Biomedical Engineering*, Vol. 39 (5), p. e3701.

[3] Richárd, W., "github.com/weberrichard/first_blood.", .

[4] Wéber, R., Viharos, M., Gyürki, D., and Paál, G., 2024, "Improvement for the hemodynamic solver, First Blood, using the MacCormack scheme", *Biomechanica Hungarica*.

[5] Bing, Y., Józsa, T. I., and Payne, S. J., 2024, "Parameter quantification for oxygen transport in the human brain", *Computer Methods and Programs in Biomedicine*, Vol. 257, p. 108433, URL https://linkinghub.elsevier.com/retrieve/pii/S0169260724004267.

[6] Nichols, W. W., O'Rourke, M. F., and Vlachopoulos, C., 2011, *McDonald's blood flow in arteries: theoretical, experimental and clinical principles*, Hodder Arnold, London, 6th ed edn., ISBN 978-0-340-98501-4.

[7] Liang, F., Takagi, S., Himeno, R., and Liu, H., 2009, "Biomechanical characterization of ventricular–arterial coupling during aging: A multi-scale model study", *Journal of Biomechanics*, Vol. 42 (6), pp. 692–704, URL https://linkinghub.elsevier.com/retrieve/pii/S0021929009000268.

[8] Fonyó Attila, Ligeti Erzsébet, Kollai Márk, and Szűcs Géza, 2008, *Az orvosi élettan tankönyve*, Medicina, Budapest, 4., átdolg., bőv. kiad edn., ISBN 978-963-226-126-3, oCLC: 909502283.

[9] Wong, J., Simmons, C., and Young, E., 2017, "Modeling and Measurement of Biomolecular Transport and Sensing in Microfluidic Cell Culture and Analysis Systems", *Modeling of Microscale Transport in Biological Processes*, Elsevier, ISBN 978-0-12-804595-4, pp. 41–75, URL https://linkinghub.elsevier.com/retrieve/pii/B9780128045954000031.

[10] El-Bouri, W. K., and Payne, S. J., 2015, "Multi-scale homogenization of blood flow in 3-dimensional human cerebral microvascular networks", *Journal of Theoretical Biology*, Vol. 380, pp. 40–47, URL https://linkinghub.elsevier.com/retrieve/pii/S0022519315002398.